Asian Journal of Chemistry; Vol. 24, No. 11 (2012), 5249-5252

ASIAN JOURNAL OF CHEMISTRY

www.asianjournalofchemistry.co.in

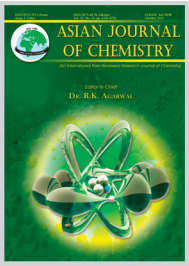

Assembled Monolayer of Silicalite-1-Supported Iron Oxide Nanoparticles for Carbon Nanotube Growth by Catalytic Chemical Vapour Deposition

WEI ZHAO[1], HYUN SUNG KIM[2], DONG NAM SEO[1], ASHISH POKHREL[1], HYUNG TAE KIM[3] and IK JIN KIM[1,*]

[1]Institute for Processing and Application of Inorganic Materials, Department of Materials Science and Engineering, Hanseo University, 360 Daegok-ri, Haemi-myun, Seosan city, Chungnam, 356-706, South Korea
[2]Center fro Nanomaterials/Korea Center for Artificial Photosynthesis, Sogang Bldg., Sogang University, 1-3 Shinsu-dong, Mapo-gu, Seoul, 121-854, South Korea
[3]Korea Institute of Ceramic Engineering and Technology, Icheon 467-84, Kyoung-gi do, South Korea

*Corresponding author: E-mail: ijkim@hanseo.ac.kr; zhao-w05@mails.tsinghua.edu.cn

(*Received*: 13 October 2011; *Accepted*: 15 June 2012) AJC-11608

An assembled monolayer of silicalite-1 microcrystals was prepared on a Si wafer for carbon nanotube grown by rubbing method. Iron oxide (α-Fe_2O_3, hematite) catalyst films were deposited onto the silicalite-1 layer from a Fe_2O_3 target by radio frequency-sputtering. This approach demonstrated the potential to produce well-aligned and diameter-controlled carbon nanotubes from predesigned silicalite-1 templates by catalytic chemical vapour deposition. The silicalite-1 monolayer oriented with faces parallel to the Si wafer showed planes only in the form of {0 k 0} lines at (020), (040), (060), (080) and (0100), according to the X-ray diffraction (XRD) results. The carbon nanotubes were formed and grown by catalytic chemical vapour deposition within the pores of the silicalite-1 crystals. These pores were consequently defined as confined channels with a pore diameter of 5.60 Å that acted as a template for a fine dispersion of well-defined Fe_2O_3 (10-15 nm) particles.

Key Words: Carbon nanotubes, Catalytic chemical vapour deposition, Silicalite-1, Assembled monolayer, Fe_2O_3.

INTRODUCTION

Carbon nanotubes are well-known as excellent thermally and electrically conductive materials due to their unique combination of large surface area and high-strength[1, 2], leading to their applications as hydrogen storage media, energy conversion devices, sensors, field emission displays, nanometer-sized semiconductor devices, interconnects for nanoelectronic devices and carbon nanotube polymeric composites for flexible electronic applications[3-5] *etc*.

For these potential applications, worldwide efforts have focused on producing high-quality single-walled carbon nanotubes and multi-walled carbon nanotubes that form around the core of single-walled carbon nanotubes by simple and reliable techniques such as arc-discharge[6], laser evaporation[7] and chemical vapour deposition, especially catalytic chemical vapour deposition[8,9].

The processes of fabricating catalysts for synthesizing vertical arrays of carbon nanotubes require vacuum deposition conditions such as the electron beam evaporation of iron. However, such methods are not as conducive to scale-up as an all-liquid phase process. In such an approach, a suitable procatalyst should be synthesized by wet chemistry techniques that can be used to control the particle diameter and composition[10]. These particles are then assembled into a two-dimensional monolayer on the catalyst support surface for the growth of vertically aligned carbon nanotubes. In principle, finely dispersed, nanometer-sized, metal particle catalysts are required to preserve their morphology at the chemical vapour deposition processing temperatures, because controlling the morphology of the catalytic particles during carbon nanotube growth strongly affects nanotube characteristics such as diameter, uniformity and yield[11].

However, as the size of the metal particles decreases to the nanometer scale, they tend to agglomerate. To prevent this, porous materials have been proposed as supports (templates)[9]. Among the catalytic supports that have been used, zeolites with pore diameters in the range of 3.0-8.0 Å have had a significant impact due to their high reactive surface areas and structural homogeneity[12]. These properties make them very suitable host candidates for different kinds of adsorbing molecules[13] and have led to their use as supports for the catalyst particles to synthesize and grow carbon nanotubes.

In this work, a well-aligned, assembled monolayer of silicalite-1 (AMS) microcrystals (5.60 Å) was deposited on a

Si wafer by rubbing and an iron oxide (α-Fe_2O_3, hematite) film was coated on the assembled monolayer of silicalite-1 substrates by radio frequency (rf)-sputtering. The finely dispersed Fe_2O_3 particles coated on porous assembled monolayer of silicalite-1 crystals were used as catalysts for the synthesis and growth of carbon nanotubes by catalytic chemical vapour deposition. The influence of the template orientation and the effect of the silicalite-1 microcrystal pore size on the synthesis and growth of carbon nanotubes was tested and analyzed.

EXPERIMENTAL

Preparation of the catalyst on assembled monolayer of silicalite-1 (AMS): A silicalite-1 monolayer was simply formed according to a previous reported procedures[14]. Briefly, silicon wafers (1 cm × 2 cm) were sonicated with absolute ethanol and dried with N_2 stream followed by oxygen plasma treatment for 5 min. A polyethylenimine solution (0.5 wt % in ethanol) was coated on the cleaned Si wafer by spin-coating. Silicalite-1 powder was spread on the coated Si wafer and gently rubbed by a clean soft latex gloved finger to avoid contamination. The rubbing method is also more effective for the monolayer assembly of silicalite-1 on large-area substrates at high speed. Fe_2O_3 films were deposited onto assembled monolayer of silicalite-1 from a Fe_2O_3 target in an rf-sputtering system for 15 min. The base pressure in the chamber before sputtering was -10^{-7} Torr. During sputtering, the Ar pressure was set to 10 mTorr at an rf power of 50 W. The structure of the catalyst for carbon nanotube synthesis is shown in Fig. 1(a).

Synthesis and growth of carbon nanotubes: The carbon nanotubes were synthesized by catalytic decomposition of C_2H_2 on the catalyst as described above in a fixed-bed flow reactor at atmospheric pressure. The reactor setup consisted of a quartz boat containing the catalyst samples, which were placed in a horizontal electric tubular furnace, as schematically shown in Fig. 1(b). The catalysts were gradually heated from room temperature to 700 and 750 ºC in a nitrogen (N_2) flow (500 sccm) and kept at this temperature for about 15 min. A mixture of N_2 (200 sccm) and C_2H_2 (10 sccm) was subsequently fed into the reactor for 1 h, in order for the reaction to proceed. The furnace was then cooled to room temperature under a N_2 flow (500 sccm) and the carbon nanotube-coated Si wafers were taken out from the quartz boat.

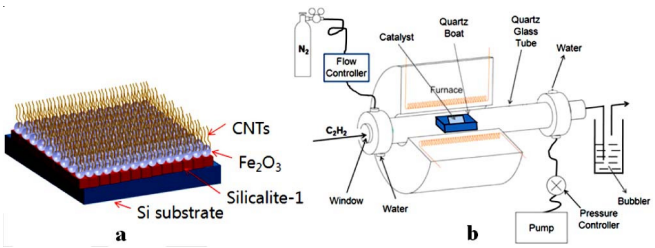

Fig. 1. Schematic representation of (a) the structure of the catalyst for carbon nanotube synthesis and (b) the water-cooled, double-wall quartz tubular furnace

The catalysts and carbon nanotubes underwent morphological characterizations by high resolution transmission electron microscopy (HRTEM, JEOL JEM-3011) at an accelerating voltage of 200 kV and field-emission scanning electron microscopy (SEM, LEO 1530 VP). Powder X-ray diffraction (XRD) experiments were performed using a Rigaku D/max 2500 VL/PC X-ray diffractometer with CuK_α (40 kV, 40 mA, k = 1.5418 Å) radiation. Raman spectroscopy measurements were performed with a Raman system FRA-106/S using a laser excitation line at 1064 nm (Nd-YAG) in the range of 200-1800 cm^{-1}.

RESULTS AND DISCUSSION

As shown in Fig. 2(a), the silicalite-1 crystals with an average size of 1.5 × 1.1 × 0.6 μm^3 were assembled onto the Si wafer in the form of a monolayer by rubbing method. Compared to the pristine synthesized silicalite-1 crystals shown with a random orientation in the inset, each coated silicalite-1 crystal was aligned with the b-axis perpendicular to the surface of the Si wafer. Despite the small size and round edge of the crystals, the rubbing procedure for assembled monolayer of silicalite-1 still worked well, as shown in Fig. 2(b). A thorough inspection of the Si wafer revealed it to be entirely covered with the monolayer of closely packed silicalite-1 crystals with only minor defects. From the inset of Fig. 2(b), the pore size on the sheet parallel to the (010) plane was measured as 5.6 Å. In the energy dispersion spectroscopy (EDX) analysis (5-10 nm), the assembled monolayer of silicalite-1-supported Fe_2O_3 particles under unchanged sputtering conditions (temperature, time, power and pressure) exhibited a fine dispersion, as shown in Fig. 2(c), suggesting that the non-continuous surface of assembled monolayer of silicalite-1 contributed significantly to particle stabilization by preventing normal sputtering [inset of Fig. 2(d)]. In addition, the large surface area and high adsorption capacity of porous supports can increase the number of dispersed particles, thus increasing the number of nucleation sites, which is advantageous for high-yield carbon nanotube growth[15].

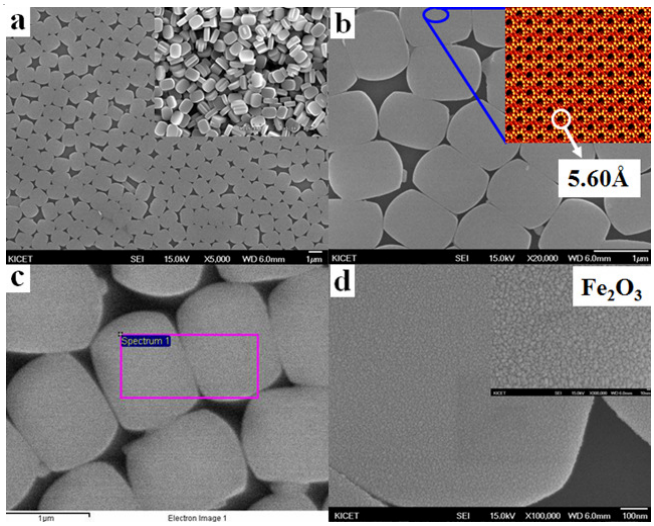

Fig. 2. (a) Low magnification SEM images of uniformly-oriented assembled monolayer of silicalite-1 microcrystals (vertical view) and pristine synthesized silicate-1 crystals (see the inset), (b) high magnification SEM image of uniformly-oriented assembled monolayer of silicalite-1 microcrystals (vertical view) and the pore structure on the (100) sheet (see the inset), (c) SEM/EDX image of Fe_2O_3 nanoparticles coated on assembled monolayer of silicalite-1 and (d) Fe_2O_3 nanoparticles (shown in the inset) coated on silicalite-1 microcrystals

In contrast to the fine particles on assembled monolayer of silicalite-1 as shown in Fig. 2(d), the Fe_2O_3 film directly deposited onto the Si wafer by rf-sputtering presented a continuous surface with large particles (-200 nm), as shown in Fig. 3(a). Fig. 3(b) shows the XRD pattern of the coated Fe_2O_3 (α-Fe_2O_3, hematite) film on the Si wafer. It is apparent that the XRD profile shows six distinguishable peaks, all of which can be perfectly indexed to an orthorhombic α-Fe_2O_3 (hematite) structure (JCPDS file no., 87-1166) with lattice parameters a = 4.59(3) Å, b = 4.97(3) Å, c = 6.68(5) Å and Z = 4. The XRD pattern of the attached silicalite-1 crystals is shown in Fig. 3(d). After the coating of the assembled monolayer of silicalite-1 crystals on the Si wafer, only (0k0) reflection planes (k = 2, 4, 6, 8 and 10) were present at 2θ = 8.9, 17.8, 26.8, 36.0 and 45.5º, respectively, due to the uniform orientation of the microcrystals. This diffraction pattern was clearly very different from that of the randomly oriented powder patterns of the silicalite-1 crystals shown in the inset of Fig. 3(d). Consistent with this result, each crystal was aligned with the b-axis perpendicular to the plane of the Si wafer on the entire substrate, as shown in Fig. 3(c).

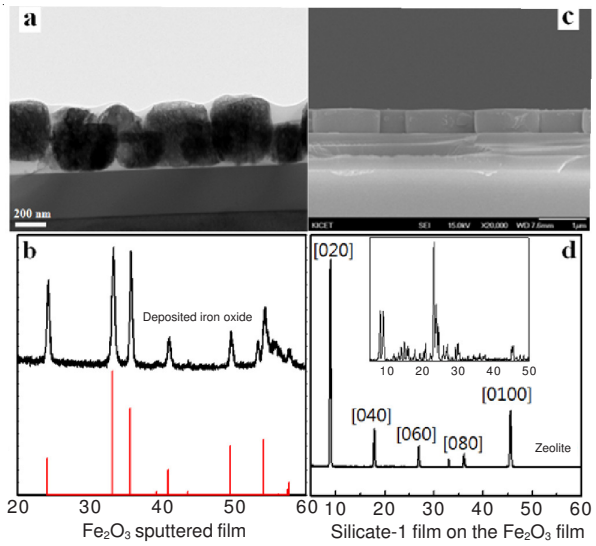

Fig. 3. (a) TEM image and (b) XRD pattern of the Fe_2O_3 film directly deposited onto the Si wafer by rf-sputtering, (c) FESEM image of assembled monolayer of silicalite-1 microcrystals coated on the Si wafer by rubbing (sectional view) and (d) XRD pattern of coated assembled monolayer of silicalite-1 microcrystals coated on the Si wafer by rubbing

The low-resolution FESEM image of the carbon nanotubes synthesized at 700 ºC for 1 h shown in Fig. 4(a) reveals a disordered film of filament-like carbon nanotubes on assembled monolayer of silicalite-1 uniformly covering a large Si substrate area. The HRTEM image [inset of Fig. 4(b)] confirms that the carbon nanotubes synthesized in our work were typically multi-walled carbon nanotubes. Combined with the image collected at higher magnification shown in Fig. 4(b), the images revealed the organization of carbon nanotubes on the assembled monolayer of silicalite-1-coated Si substrate to be low-density tangles of transparent carbon nanotubes with inner and outer diameters of around 6.0 ± and 14.0 ± nm, respectively and lengths in the range of hundreds of nanometers or even several micrometers[16].

Fig. 4(c) shows a low-resolution FESEM image of the carbon nanotubes synthesized at 750 ºC for 1 h. Similar to those synthesized at 700 ºC, the synthesized carbon nanotubes were multi-walled carbon nanotubes in the form of a thick carpet clearly evident on the assembled monolayer of silicalite-1-coated Si substrate. The high magnification FESEM image [Fig. 4(d)] and the HRTEM image [inset of Fig. 4(d)] show tangles of transparent carbon nanotubes on the assembled monolayer of silicalite-1-coated Si substrate with inner and outer diameters of approximately 10.0 ± and 26.0 ± nm, respectively and lengths in the micrometer range[16].

The sectional view of synthesized carbon nanotubes on the assembled monolayer of silicalite-1-coated Si substrate was also investigated. The FESEM image [Fig. 4(e)] shows the as-grown carbon nanotubes on assembled monolayer of silicalite-1 crystals. Most silicalite-1 crystals were surrounded by the filaments, with some being already oriented in the vertical direction. The ensemble of these carbon nanotubes resembled bloomy flowers. However, the surface of the assembled monolayer of silicalite-1 crystals was not completely covered by carbon nanotubes, possibly due to the coalescence of some Fe_2O_3 nanoparticles. Although Fe_2O_3 has an ultra-high activity for C_2H_2 decomposition and the subsequent formation of a carbon nanotube over-layer at relatively low temperature, it is still not favourable for carbon nanotube synthesis during the pretreatment prior to feeding C_2H_2.

The quality of the multi-walled carbon nanotubes was investigated using Raman spectroscopy. Fig. 4(f) shows typical D- and G- bands, centered at 1295 and 1590 cm^{-1}, indicating the presence of crystalline graphite carbon and impurities and dispersive defects in the graphitic sheets[17], respectively. The I_D/I_G intensity ratio, which is used as a measure of the degree of disorder in the graphite sheets, increased from 7.2 for carbon nanotubes synthesized at 700 ºC to 8.7 for those synthesized at 750 ºC, indicating a higher disorder for carbon nanotubes synthesized at 750 ºC. This result was confirmed by the presence of two peaks at frequencies of 1060 (T peak) and 1332 cm^{-1} representing amorphous carbon[18] and the diamond sp^3 peak[19], respectively, as revealed by the comparison between Figs. 4(b) and 4(d).

Conclusion

Fe_2O_3 catalysts (α-Fe_2O_3, hematite, a = 4.59(3) Å, b = 4.97(3) Å, c = 6.68(5) Å, Z = 4) deposited by rf-sputtering on well-aligned assembled monolayer of silicalite-1 microcrystals that had themselves coated on a Si wafer substrate by rubbing were prepared for the formation and growth of carbon nanotubes by catalytic chemical vapour deposition. XRD results indicated that the silicate-1 monolayer oriented with faces parallel to the Si substrate showed planes only in the form of {0 k 0} lines at (020), (040), (060), (080) and (0100). The carbon nanotubes were formed and grown by catalytic chemical vapour deposition within the pores of the assembled monolayer of silicalite-1 crystals. Consequently, these pores were defined as confined channels of nanometer dimensions that acted as a template for the carbon nanotube growth, because some of the carbon nanotubes already showed a vertical growth tendency. In addition, the carbon nanotube diameters increased at higher temperature (750 ºC) as they became increasingly disordered with more defects.

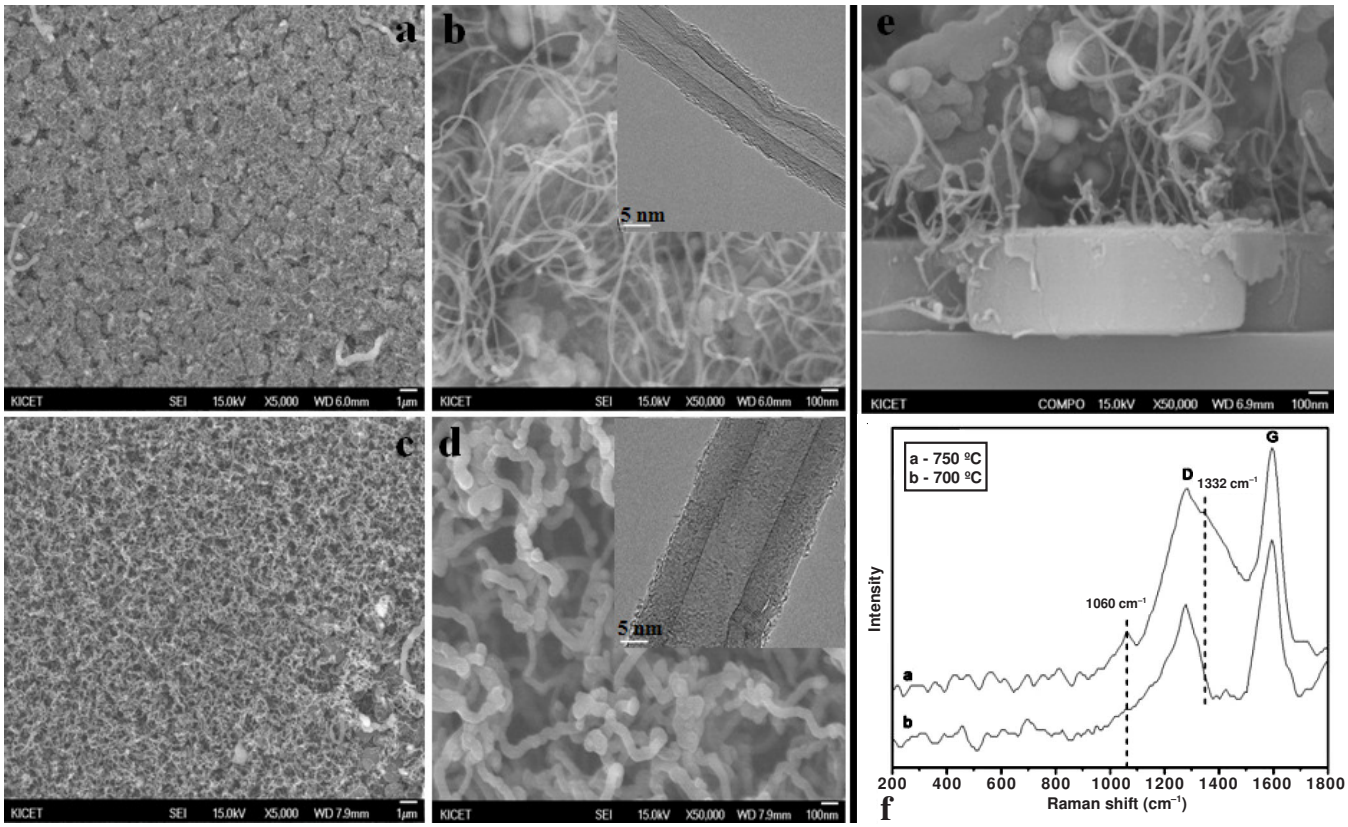

Fig. 4. (a) Low-resolution FESEM image of carbon nanotubes synthesized at 700 ºC, (b) high-resolution FESEM image of carbon nanotubes synthesized at 700 ºC with the inset showing HRTEM image of synthesized carbon nanotubes, (c) low-resolution FESEM image of carbon nanotubes synthesized at 750 ºC, (d) high-resolution FESEM image of carbon nanotubes synthesized at 750 ºC with the inset showing HRTEM image of synthesized carbon nanotubes, (e) high-resolution FESEM image of carbon nanotubes (sectional view) on iron oxide supported on assembled monolayer of silicalite-1 and (f) Raman spectroscopy of carbon nanotubes synthesized at 700 and 750 ºC for 1 h

ACKNOWLEDGEMENTS

This work was supported by the Research Foundation from Hanseo University in 2011. The authors are grateful to all staff in the university for financial support.

REFERENCES

1. C. Yu, L. Shi, Z. Yao, D. Li and A. Majumdar, *Nano Lett*., **5**, 1842 (2005).
2. M. Fuhrer, H. Park and P. L. McEuen, *IEEE Trans, Nanotechnol.*, **1**, 78 (2002).
3. J. Li, Q. Ye, A. Cassell, H.T. Ng, R. Stevens and J. Han, *Appl. Phys. Lett.*, **82**, 2491 (2003).
4. J.K. Holt, H.G. Park, Y. Wang, M. Stadermann, A.B. Artyukhin, C.P. Grigoropoulos, A. Noy and O. Bakajin, *Science*, **312**, 1034 (2006).
5. Y.J. Jung, S. Kar, S. Talapatra, C. Soldano, G. Viswanathan, X. Li, Z. Yao, F.S. Ou, A. Avadhanula, R. Vajtai, S. Curran, O. Nalamasu and P.M. Ajayan, *Nano Lett.*, **6**, 413 (2006).
6. T.W. Ebbesen and P.M. Ajayan, *Nature*, **358**, 220 (1992).
7. T. Guo, P. Nikolaev, A.G. Rinzler, D. Tomanek, D.T. Colbert and R.E. Smallery, *J. Phys. Chem.*, **99**, 10694 (1995).
8. M. Endo, K. Takeuchi, K. Kobori, K. Takahashi, H.W. Kroto and A. Sarkar, *Carbon*, **33**, 873 (1995).
9. H. Ago, S. Imamura, T. Okazaki, T. Saitoj, M. Yumura and M. Tsuji, *J. Phys. Chem.*, **B109**, 10035 (2005).
10. N.T. Alvarez, A. Orbaek, A.R. Barron, J.M. Tour and R.H. Hauge, *Appl. Mater. Interfac*., **2**, 15 (2010).
11. T. Yamada, T. Namai, K. Hata, D.N. Futaba, K. Mizuno, J. Fan, M. Yudasaka, M. Yumura and S. Iijima, *Nat. Nanotechnol.*, **1**, 131 (2006).
12. I.J. Kim, W. Zhao, X. Fan, J.H. Chang and L.J. Gauckler, *J. Ceram. Res. Proces.*, **11**, 158 (2010).
13. S. Karakoulia, L. Jankovic, K. Dimos, D. Gournis and K. Triadafyllidis, *Stud. Surf. Sci. Catal.*, **158**, 391 (2005).
14. J.S. Lee, J.H. Kim, Y.J. Lee, N.C. Jeong and K.B. Yoon, *Angew. Chem. Int.*, **46**, 3087 (2007).
15. K.B. Yoon, *Acc. Chem. Res*., **40**, 29 (2007).
16. S. Yasuda, D.N. Futaba, T. Yamada, J. Satou, A. Shibuya, H. Takai, K. Arakawa, M. Yumura and K. Hata, *ACS Nano*, **3**, 4164 (2009).
17. L.D. Shao, G. Tobias, C.G. Salzmann, B. Ballesteros, S.Y. Hong, A. Crossley, B.G. Davis and M.L.H. Green, *Chem. Commun.*, 5090 (2007).
18. A.C. Ferrari and J. Robertson, *Phys. Rev. B*, **64**, 075414 (2001).
19. A.C. Ferrari and J. Robertson, *Phys. Rev. B*, **63**, 121405 (2001).